Hybrid Control in Automotive Applications

A. Balluchi, M.D. Di Benedetto, C. Pinello, A. Sangiovanni–Vincentelli [1]

Abstract

Hybrid systems have captured the attention of the research community because of their intrinsic power and of the challenging mathematical problems they pose. We believe that much needs to be done to understand how to use effectively this mathematical formalism for important applications. We have embarked on an ambitious project aiming at the complete redesign of an automotive engine control unit for the next generation automobiles equipped with complex devices such as drive-by-wire and electronic valve control. The design problem has been formulated in an innovative way and makes extensive use of hybrid system technology. We present first the overall methodology and its basic components. Then we focus on the highest levels of abstraction that involve the formulation of the control problem and its solution. A hybrid model which describes the torque generation mechanism and the powertrain dynamics is developed. Then, two particular control sub-problems (cut-off and fast positive force tracking) are formulated as hybrid optimal control problems, whose solutions are obtained by relaxing the problems to the continuous domain and mapping their solutions back into the hybrid domain. A formal analysis as well as experimental results demonstrate the properties and the quality of the control laws.

1 Introduction

1.1 The Framework

Hybrid systems have been the subject of intensive study in the past few years with particular emphasis placed on a unified representation of the models in terms of rigorous mathematical foundations (see [12], [19], [15], [14], [8], [9]). The class of hybrid control problems is extremely broad since it obviously contains continuous control problems as well as discrete event control problems as special cases. For this reason, it is very difficult to devise a general yet effective strategy to solve such problems. In our opinion, it is important to address significant domains of application of hybrid control to develop further understanding of the implications of the model on the control algorithms.

In this paper, we focus on a domain of application that is of great industrial interest: automotive engine control. In this domain, the ever increasing computational power of micro–controllers has made it possible

[1] Research sponsored in part by a CNR grant

to extend the performance and the functionality of electronic sub–systems controlling the motion of the car. This opportunity has exposed the need for control algorithms with guaranteed properties that can reduce substantially emission and gas consumption while maintaining the performance of the car [18, 5, 12]. We argue that most of the engine control problems are hybrid since the behavior of four–stroke gasoline engines is determined by the combination of a discrete event sub-system modeling the torque generation process, and a continuous time sub-system modeling the powertrain behavior. It is then the plant to be controlled that is hybrid, no matter what the control strategy is. This is an important point to make since some interesting general approaches to hybrid control assume that the plant to be controlled has a continuous dynamics and hence they are not directly applicable here [13, 10, 7].

The design problem addressed with the proposed approach can be described as follows. From a set of specifications given by a car manufacturer to the embedded system provider:

- find a set of algorithms that control the engine to match the specifications;
- implement the algorithms on a mixed mechanical-electrical architecture consisting of programmable components, such as microprocessors and DSP's, application specific integrated circuits, and physical devices such as sensors and actuators.

In current practice, the implementation architecture of the electronic component is fixed a priori (micro-controllers with fixed-point arithmetic units). The specifications and the control algorithms are so much tuned to this architecture that it becomes very difficult to verify in an effective way the behavior of the system. In addition, the control algorithms are based on simple, intuitive and often open loop rules. Our team embarked on an ambitious project whose goal has been to redefine the entire design process according to these principles:

- the specifications are given at a high level of abstraction so that they are independent of implementation decisions;
- the control algorithms are designed so that formal correctness and optimality properties are ensured by a rigorous mathematical framework;
- the abstract representation of the design is mapped to an architecture using estimation techniques that guide the selection process;
- the implementation architecture of the electronic component is selected among a set of candidates (e.g. a 32-bit micro-controller with Floating Point Unit, a 32-bit micro-processor with a DSP co-processor,

a multiprocessor architecture with an 8-bit I/O processor and a 16-bit micro-controller with a DSP unit) in such a way that cost, reliability and time to market are optimized.

The goal of the presented design process is to shorten the design cycle (now of the order of 5 years) by a very sizable amount (by 3 years and more!) while reducing the cost of the electronic system and increasing its quality and functionality. The conscious reuse of previously designed blocks and the capability of taking decisions at early stages of the design process are key points to this end. Our approach has been tuned and tested on industrial problems and is the result of a long standing working relationship with Magneti-Marelli, a large European automotive electronic subsystem provider.

1.2 Design methodology overview

The design process, shown in figure 1, is described as a set of successive refinement steps from a level of abstraction as high as possible all the way down to the details needed for the final implementation. The process has been conceived to be applicable in almost all embedded design problems; however, to be more concrete, we will use the Engine Control Sub-system design to illustrate the basic principles. In our approach, we identify five main levels of abstraction:

System level. At this level, the specifications are captured and analyzed. The supplier and the customer (in the case of the engine control unit, a car manufacturer) in general agree upon the specifications. The system "car" is viewed as the system converting the driver's commands conveyed by a variety of input devices such as clutch, gas and brake pedals, gear stick, cruise control settings, into actual motion and other outputs of interest to the driver or to some regulatory body, (governments or car manufacturers associations) such as emission levels, noise, fuel consumption. Constraints are placed on these outputs and objective functions are set to determine the quality of the car as specified by market analyses performed by the car manufacturer. According to the market segment targets, a car in the high-performance range will be required to respond to a fast push of the accelerator pedal within a very short time, with little regard to the fuel consumption needed to achieve this goal, while an economy car will be required to respond as well as possible to the command maintaining the fuel consumption below a certain threshold. Since some of the key mechanical components of the car, such as the engine and the chassis, are in general not part of the embedded system design, they can be considered as given. Thus, the goal is to design the engine control sub-system so that the car with that particular engine and chassis performs as specified. Unfortunately, most often than not, the specifications are determined according to an informal process that leads to misunderstanding and late product delivery. To support precise specifications, a simulation environment together with an engineering spreadsheet tool is highly desirable and is being developed in collaboration with Cadence Design Systems, Inc.

Function level. Once the specifications are determined, the design process inside the supplier company begins. Because of the complexity of the problem, a decomposition of the system into interacting simpler subsystems, called functions, is clearly a key step towards a good quality design. The decomposition is useful if it leads to a design process that can be carried out as independently as possible for each component. The decomposition process has to "spread" constraints and objectives among the components so that the composition of the behaviors of the components, made feasible and possibly optimal with their own constraints and cost functions, is guaranteed to meet the constraints and the objectives of the overall controlled system. Since in general it is difficult to decompose the system into independent parts, the determination of the local objectives and constraints has to be the result of a careful trade-off between the desire of maintaining optimality at the global level and the one of easing the design task for each of the components considered in isolation. This decomposition has to be based on the understanding of the physical process of interest. For the engine control case, the variables to be controlled are the air-fuel mix, the injection timing and the spark timing while the objective and constraints are stated in terms of emissions and motion of the car. Motion is the result of the application of torque to the driveline. The engine, via the combustion process, produces the torque. Emissions are the result of the chemical process in the catalytic converter that is fed the exhaust gases of the combustion process. The combustion process in turns is controlled by the quantities introduced above. The air-fuel mix is the result of two processes each determining the air and fuel quantity to mix. From this simple analysis, it appears that motion generation and emission generation are the results of a cascade of chemical-electrical-mechanical processes and that each can be controlled somewhat independently once the local constraints and objectives are set. In Section 3, we will present this example with more details.

Operation level. Once the decomposition of the problem has been performed, each sub-problem has to be solved with its constraints and objectives. Each sub-problem solution is expressed in terms of basic building blocks, called operations, for re-use. Each operation is given a classification in terms of its nature, e.g., measurement, actuation, and control operations. At this level, we start deciding "how to solve" the problem while at the system and function level we were dealing with "what is the problem" to solve. If, indeed, one or more of these sub-problems are not solvable, we need to revisit the previous design step to adapt the local objectives and constraints or to change the decomposition itself. Note that we try to close the design loop as early as possible to avoid major re-design steps at a later stage that can yield so much damage to schedule and profitability.

Architecture level. The operations are still defined abstractly and not directly related to physical devices. At the architecture level, we determine the actual interconnection of components (architecture) that implement one or more operations. This step consists of matching abstract operations with a collection of available or "to-be-designed" devices trying to optimize cost, size, reliability, time-to-market. Components can be classified as electrical, chemical, or mechanical devices. Some examples of components are the pressure sensor, the intake manifold, and the microprocessor. Note that the microprocessor or any other software programmable component is very flexible since it can be used to implement a large class of operations. At this level, the actual performance of the system can be more precisely estimated. If the estimation indicates that the objectives and constraints are not met, the choice of operations has to change accordingly. Once more the engineering change loop is closed as early as possible.

Component level. This step involves the actual design of the components of the architecture determined in the previous step if they are not available in the library or if their use requires some degree of customization as in the case of electronic programmable components, where software must be developed to customize the processor for the particular operation under consideration.

The operation and architecture design process is tightly linked. Decisions taken on what operations to implement have an obvious impact on the architecture and vice-versa. Hence it is very difficult to de-couple these two steps. Indeed, the mapping process from operations to architecture is critical to obtain a good design. In our methodology, mapping is performed continuously so that cost and performance estimation can guide the design decisions.

Note that operation and architecture abstractions are shown in parallel to stress that the two design processes have to be tightly linked. It is in this phase that we address the key problem of software design. Software is the by-product of mapping a set of operations to the programmable components of the electronic architecture. In summary, the overall methodology is hierarchical and consists of five main levels and of the mapping steps that take from one level to the next. Each step is characterized by analysis and optimization that can be carried out with the appropriate tools. The goal is to make the design process rigorous and as well defined as possible and to re-use as much as possible any of the design components for the present application as well as for future applications.

1.3 Paper organization

The focus of this paper is on the various aspects of the mathematical models used to represent the engine and the power-train and of the design of the control algorithms. A companion paper describes the main issues related to algorithm implementation and architecture selection [11]. In particular, the paper is organized as follows. In Section 2, the way we construct the reference model for the engine control problem is described. In Section 3, the torque–generation and powertrain models are presented as hybrid systems. In Section 4, a control sub-problem related to the region of operation of the engine when the driver pushes quickly the accelerator pedal, is formulated and solved in the hybrid system domain. The strategy is to first find an optimal solution to the continuous time relaxed control problem and then to map it back in the hybrid domain. In Section 5, another sub-problem is considered related to the region of operation of the engine when the driver releases quickly the accelarator pedal. For cars equipped with drive-by-wire subsystems, this problem can be formulated as a minor variation of the previously considered problem. However, a substantial difference exists if the throttle angle is not available as a control variable. In this case, we devised a strategy, following the same general ideas, that yields a solution demonstrably close to the upper bounding optimal solution to the relaxed problem. Some concluding remarks are offered in Section 6.

2 System behavior specifications: constructing the reference model

A car manufacturer gives the system specifications in terms of how the vehicle should react to the inputs given by the driver. In this paper, we restrict our attention to the specifications related to force requests, i.e. we do not deal with requirements on trajectory control of the vehicle. The assumption is that the driver requests force by using the gas, brake and clutch pedals, and a manual gear shift. In general, the capture of the specifications as interpreted by the supplier is often obscured by other considerations involving the implementation of a system, thus making it difficult to re-use part of the solution as well as to verify whether the specifications are met. In our approach, the specifications are captured using a hybrid model as shown in figure 1. The states of the top-level Finite State Machine (FSM) correspond to different regions of operations of the engine. The transitions are determined by the action of the driver on the input signals or by engine conditions. Each region of operation is characterized by a set of constraints related to driving performance, such as comfort and safety, or gas and noise emission, and a cost function that identifies the desired behavior of the controlled system. The controlled system is represented by a model that includes ordinary differential equations as well as discrete components. The goal of the controller is to act on the inputs to the plant (the throttle plate angle, the injection pulse duration and the spark advance angle) so that it behaves according to the specifications summarized in the FSM. Figure 1 shows the FSM that specifies the behavior of the vehicle. The initial state is the Stop state that corresponds to the engine being off. From this state, the driver causes the transition to the Startup state, turning the ignition Key to the startup value. From the Startup state the FSM enters the Idle state, if the gas pedal signal is 0, otherwise enters the RPM Tracking state. The desired behavior of the controlled system in the Idle state, for example, is the following: the force F_G acting on the vehicle has to be zero and the crankshaft revolution speed n must be regulated to a reference value, e.g. 500 rpm, with an excursion of up to 20 rpm while minimizing fuel consumption. Moreover, the transient response with respect to sudden loads of 25 Nm must have a 'settling time' of 2 s and an excursion less than 40 rpm. Last, the air-fuel ratio must remain within (10/00 of the stoichiometric desired level). In the RPM Tracking state, the engine is supposed to adjust its RPM to match a prescribed relationship with the gas pedal signal. When the transmission is engaged, the Force Tracking state is entered. In this state, a particular torque profile, that depends on the gas pedal position, the gear and the RPM, has to be realized with constraints on the settle time and with cost function related to fuel consumption and drive comfort.

The Fast Negative Force Transient (FNFT) state is entered if the gas pedal is suddenly released. In this state, a step reference for the requested force is considered and a different control law is used. This control law should minimize the transient time subject to very tight drive comfort constraints. However, if no drive-by-wire control is available, a feasible solution may not exist. In this case, the optimization problem is reformulated so that the driving comfort constraint becomes the cost function. When the gas pedal is pushed again or the transient is elapsed, the transition to the Force Tracking (FT) state is entered. If the gas pedal is completely released and the minimum RPM is approached, the transition to the Idle with transmission on state is enabled. In this state, the RPM is kept constant at a prescribed value until the gas pedal position or the RPM triggers the transition to the Force tracking state. If the gas pedal is pushed quickly, then the transition to the Fast Positive Force Transient (FPFT) state is enabled. This state is the mirror image of the FNFT state. Here the torque profile to be followed is a positive step and the control law minimizes the transient time subject to fuel consumption and comfort constraints. Finally, when a cruise control is available, a Speed Tracking (ST) state is present. If the driver turns the Key to the stop value or if the engine turns off, the Stop state is reached. Although this scheme is very simple, it has quite an impact in clarifying

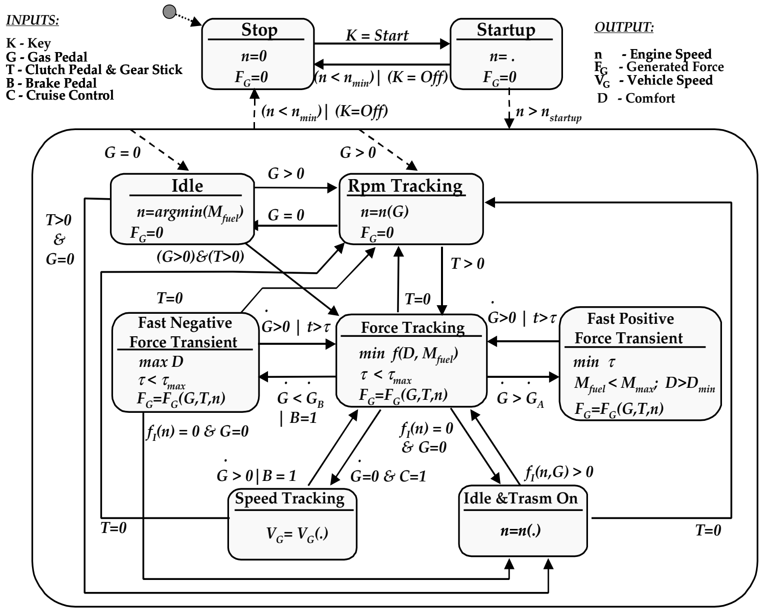

Figure 1: FSM of the regions of operation describing system specifications.

the objectives of the design and how to decompose the problem into well defined sub-problems. In addition, this way of specifying the problem has an impact on the final implementation, reducing the amount of complexity and redundancy in the code. The requirements captured by the diagram can be considered as the specifications for the control problem. In addition, the structure of the FSM is the same independently of the car manufacturer or of the car range. Only the parameters of the cost and constraint functions change, thus favoring maximum re-use.

3 Plant model

In this section, the hybrid model proposed in [2][3] for vehicles with 4–stroke N–cylinder gasoline engine is illustrated. The hybrid model $\mathcal{M}_{1cyl}$ of a vehicle with single cylinder engine is reported in Figure 2. This model is composed of three parts:

1. a Finite State Machine[2](FSM) describing the behavior of the pistons;

[2]A deterministic Finite State Machine is a six-tuple $M = \{I, Y, \mathcal{S}, s_0, \lambda, \gamma\}$ where I is the (finite) set of inputs, Y is the (finite) set of outputs, $\mathcal{S}$ is the finite set of states, s_0 is the initial state, $\lambda : \mathcal{S} \times I \to \mathcal{S}$ is the next state function, $\gamma : \mathcal{S} \times I \to Y$ is the output function.

2. a Discrete Event system[3](DE) modeling torque generation (dashed boxes and lines);

3. a Continuous Time (CT) system modeling the powertrain and air dynamics (solid boxes and lines).

The combination of the FSM and the DE system describes the torque generation mechanism for a single cylinder, whose behavior is affected by the CT powertrain and air evolution. The hybrid model for a N-cylinder vehicle is obtained composing N FSM/DE cylinder models and the CT model.

Powertrain Model. The powertrain is described by a continuous time system model developed, identified and validated at Magneti Marelli Engine Control Division. Powertrain dynamics are modeled by the linear system

$$\dot{\zeta} = A\,\zeta + b\,u - b_0 \quad (3.0.1)$$
$$\dot{\phi}_c = [0,\ 1,\ 0]\,\zeta \quad (3.0.2)$$
$$a = c\,\zeta - d_0 \quad (3.0.3)$$
$$j = (cA)\,\zeta + (cb)\,u - (cb_0) \quad (3.0.4)$$

Where $\zeta = [\alpha_e, \omega_c, \omega_p]^T$ represents the axle torsion angle, the crankshaft revolution speed, the wheel revolution speed, and the 4–th variable ϕ_c represents the crankshaft angle. The input signal u is the torque produced by the engine and acting on the crankshaft. Vector b_0 models the resistant actions on the powertrain, due to both internal friction and external forces. Dynamics (3.0.1) is asymptotically stable and is characterized by a real dominant pole λ_1, and a pair of conjugate complex poles $\lambda \pm j\mu$. Vehicle acceleration (3.0.3) and jerk (3.0.4) ($j = \frac{da}{dt}$) are the powertrain outputs of interest for drivability and comfort. Assuming vehicle speed equal to wheel speed and denoting by R_w the wheel radius, we have $a = R_w\dot{\omega}_p = R_w[0,0,1](A\zeta + bu - b_0)$, and since the third entry in b is 0, $a = R_w[0,0,1]A\zeta - R_w[0,0,1]b_0$, i.e. $c = R_w[0,0,1]A$, $d_0 = R_w[0,0,1]b_0$. Model parameters A, b, c, b_0 and d_0 depend on the transmission gear, and it is assumed that, during a cut–off operation, the driver does not act on the gear.

Cylinder's behavior. The behavior of each cylinder in the engine is abstractly represented by the Finite State Machine shown in Figure 2. FSM state $\mathcal{S}$ assumes values in the set $\{H, I, C, E\}$ as follows.

- *Exhaust run* represented by state H. The piston goes up from the bottom to the top of its run (bottom and top dead centers resp.), expelling combustion exhaust gases.

[3]A DE system is intended in the sense of [11].

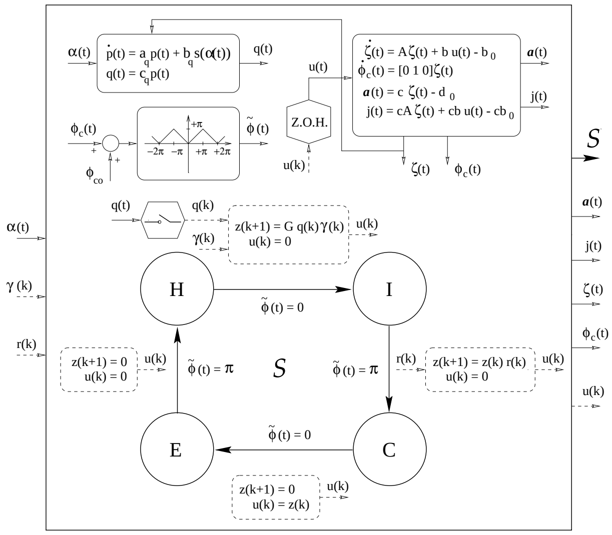

Figure 2: Hybrid model for a vehicle with 4–stroke single cylinder engine.

- *Intake run* represented by state I. During its down–run the piston loads the air–fuel mix.
- *Compression run* represented by state C. During its up movement the piston compresses the loaded mix.
- *Expansion run* represented by state E. The compressed mix combustion, generated by a spark signal, produces a sudden pressure increase which pushes the piston downwards.

The transitions occur when the piston reaches the bottom or top dead center. The guard conditions enabling the transitions in the FSM are written in terms of the piston position expressed by $\tilde{\phi}$: the absolute value of the crank angle with respect to the upper dead center position, related to the crankshaft angle ϕ_c as depicted in Figure 2, where ϕ_{co} corresponds to the angle the crank is mechanically mounted on the shaft.

Torque generation. The timing of the spark can be set at each cycle in order to modulate the generated torque (see [2] [4]). Moreover this process is characterized by the delays between the times in which fuel injection and spark advance are set and the time in which such decisions have an effect. Control signals are then subject to a transport process which can be represented by a DE system active at every FSM transition. Such DE system, reported in Figure 2 with dashed boxes, increments its time counter

k by one at each transition. Its inputs are: the mass of air-fuel mix $q(k) \in \mathbb{R}^+$ loaded during the intake phase; a parameter $\gamma(k) \in [\gamma_{\min}, \gamma_{\max}]$ which represents the ratio between the mass of fuel injected and the mass of air loaded, normalized with respect to its "optimal" value in reference to burning efficiency; the modulation factor $r(k) \in [r_{min}, 1]$ due to not optimal spark timing. The DE system output is the torque $u(k)$.

At the FSM transition $E \rightarrow H$ the DE system reads its inputs $q(k)$ and $\gamma(k)$, and stores in its state $z \in \mathbb{R}$ the maximum amount of torque achievable during the next expansion phase, obtained by the mix-to-torque gain G. Such value is corrected at the $I \rightarrow C$ transition applying the modulation factor $r(k)$, due to the chosen spark advance. The DE output $u(k)$ is always zero except at the $C \rightarrow E$ transition when it is set to the value stored in z. Input $u(t)$ to the CT powertrain dynamics is obtained from $u(k)$ by a zero order hold block, i.e. between two transitions of the FSM occurring at times t_k and t_{k+1}, it holds $u(t) = u(k)$ for $t \in [t_k, t_{k+1})$.

Air dynamics. The model of the quantity of air entering the cylinder during the intake run is obtained from the air flow balance equation of the manifold. Manifold dynamics is a continuous time process controlled by the throttle valve that changes the effective section of the intake manifold. The air mass loaded during an intake run from $t = t_k$, is subject to manifold pressure dynamics. Let p and α denote the manifold pressure and the throttle angle, respectively. Pressure dynamics is modeled as:

$$\dot{p} = a_q(\omega_c, p)\, p + b_q(p) s(\alpha) \tag{3.0.5}$$

$$q = c_q(\omega_c, p)\, p \tag{3.0.6}$$

where $s(\alpha)$ is the so called equivalent throttle area, given in terms of throttle angle α, and

$$a_q(\omega_c, p) = -\frac{V_d}{4\pi V_c} \eta_v(\omega_c, p)\, \omega_c, \tag{3.0.7}$$

$$b_q(p) = \frac{p_{atm}\sqrt{R_g T_{atm}}}{V_c} \beta\left(\frac{p}{p_{atm}}\right), \tag{3.0.8}$$

$$c_q(\omega_c, p) = \frac{V_d}{4 R_g T_{atm}} \eta_v(\omega_c, p) \tag{3.0.9}$$

where V_d, V_c are respectively the displacement and the displacement plus manifold volume, p_{atm}, T_{atm} are the ambient pressure and air temperature, R_g is the ideal gas constant. The volumetric efficiency in cylinder intakes is denoted by $\eta_v(\omega_c, p)$. Finally,

$$\beta\left(\frac{p}{p_{atm}}\right) = \begin{cases} \sqrt{\frac{2c_v/c_p}{c_p/c_v-1}\left[\left(\frac{p}{p_{atm}}\right)^{\frac{2}{c_p/c_v}} - \left(\frac{p}{p_{atm}}\right)^{\frac{c_p/c_v+1}{c_p/c_v}}\right]} \\ \qquad \text{if } \frac{p}{p_{atm}} \geq \left(\frac{2}{c_p/c_v+1}\right)^{\frac{c_p/c_v}{c_p/c_v-1}} \\ \sqrt{c_p/c_v}\left(\frac{2}{c_p/c_v+1}\right)^{\frac{c_p/c_v+1}{2(c_p/c_v-1)}} \\ \qquad \text{if } \frac{p}{p_{atm}} < \left(\frac{2}{c_p/c_v+1}\right)^{\frac{c_p/c_v}{c_p/c_v-1}} \end{cases}$$

While in the past throttle valve was directly connected to the gas pedal, in the future most cars will be equipped with drive–by-wire where the throttle valve is controlled by the engine control unit to achieve better performance. In this paper, we consider the case of cars equipped with drive-by-wire and for the FNFT region of operations, we also consider the case of traditional cars.

Engine hybrid model. An engine is characterized by the number of cylinders[4]. The pistons are connected to the crankshaft, so that the phases of their behavior are related to each other. The overall model of torque generation for a N–cylinder engine is then the combination of N FSMs as in Figure 2 and of N DE systems representing the behavior of each piston. The hybrid model of the complete engine is obtained by adding to torque generation model the powertrain CT dynamics (3.0.1), (3.0.2) and air CT dynamics (3.0.5) which are shared among all cylinders.

In this paper we focus on the most relevant case of a 4-cylinder engine. Its model, referred to in the rest of the paper as $\mathcal{M}_{4cyl}$, has input signals

1. throttle angle α, a scalar continuous time signal in the class $\mathcal{A}_{4cyl}$ of functions $\mathbb{R}^+ \to [0, \frac{\pi}{2}]$;
2. parameters $\boldsymbol{\gamma} = [\gamma_1, \gamma_2, \gamma_3, \gamma_4]^T$, a four dimensional discrete time signal in the class $\mathcal{G}_{4cyl}$ of functions $\mathbb{N} \to (\gamma_{\min}, \gamma_{\max})^4$, with components synchronized with the corresponding DE model;
3. spark advance modulation factors $\mathbf{r} = [r_1, r_2, r_3, r_4]^T$, a four dimensional discrete time signal in the class $\mathcal{R}_{4cyl}$ of functions $\mathbb{N} \to (r_{\min}, 1)^4$, with components synchronized with the corresponding DE model;

In a 4-cylinder engine, no FSM is in the same state at any time and all transitions are synchronous, i.e., offset angles ϕ_{c0_i} are either 0 or π. Without loss of generality, we assume that in the model $\mathcal{M}_{4cyl}$ the crankshaft offsets ϕ_{co_i} are $\phi_{c0_1} = \phi_{c0_3} = \pi, \phi_{c0_2} = \phi_{c0_4} = 0$.

[4]Most cars have four cylinders, but there are engines that have a different number of cylinders. For example, Formula 1 racing cars can have 8, 10 or 12 cylinders. Fiat Coupè 2000 Turbo has 5.

4 Fast Positive Force Transient design

4.1 The Fast Force Transient (FFT) optimal control problem

In the Fast (both Positive and Negative) Force Transient (FFT) regions of operation the objective is to steer the system from a given point, characterized by torque delivered to the crankshaft $u(0) = u_0$, to a new point with torque value u_R in minimum time. Since we consider drive-by-wire subsystems, available controls are: air mass that depends on the throttle angle, fuel injection and spark advance. The control action has to be designed so that comfort is maintained. "Peak–to–peak" acceleration and jerk have been experimentally identified as the most important factors in passenger comfort. We formulated the control problem as: *steer the powertrain elastic state, keeping the jerk within the bounds* $[0, j_{\max}]$, *to a point such that the application of the new requested value of transmitted torque produces an oscillating acceleration evolution* $\tilde{a}(t)$ *bounded above by a threshold of perception* $\tilde{a}_{th} > 0$. The oscillating acceleration evolution is computed using natural mode decomposition. Introduce

$$\begin{bmatrix} x' \\ x \end{bmatrix} = N_{\zeta x} \left(\zeta + A^{-1} b \, u_R - A^{-1} b_0\right) , \qquad (4.1.10)$$

with $x' \in \mathbb{R}$, $x \in \mathbb{R}^2$ and $N_{\zeta x} \in \mathbb{R}^{3\times 3}$ obtained from the eigenvectors of A, and input transformation $v = u - u_R$. Dynamics (3.0.1) becomes

$$\begin{bmatrix} \dot{x}' \\ \dot{x} \end{bmatrix} = \begin{bmatrix} \lambda_1 & 0 \\ 0 & A_x \end{bmatrix} \begin{bmatrix} x' \\ x \end{bmatrix} + \begin{bmatrix} b_{x'} \\ b_x \end{bmatrix} v , \qquad (4.1.11)$$

with $A_x = \left[\begin{smallmatrix} \lambda & -\mu \\ \mu & \lambda \end{smallmatrix}\right]$, and (3.0.3) is rewritten as $a = -cA^{-1}(bu_R - b_0) + [c_{x'} \; c_x] \left[\begin{smallmatrix} x' \\ x \end{smallmatrix}\right]$ with $[c_{x'} \; c_x] = c\, N_{\zeta x}^{-1}$. Under constant control v in (4.1.11), the oscillating component of the acceleration can then be expressed as

$$\begin{aligned} \dot{x} &= A_x x + b_x v , && (4.1.12) \\ \tilde{a} &= c_x x . && (4.1.13) \end{aligned}$$

Let $\hat{\rho} = \tilde{a}_{th} \| c_x^T \|^{-1}$. Consider the manifold

$$\mathcal{C}_x = \left\{ \begin{bmatrix} x' \\ x \end{bmatrix} \in \mathbb{R}^3 \,|\, x' \in \mathbb{R},\ x = \hat{\rho} \begin{bmatrix} \cos(\theta) \\ \sin(\theta) \end{bmatrix} \text{ with } \theta \in [0, \pi) \right\} \qquad (4.1.14)$$

Note that the norm of $x(t)$ in (4.1.11) decreases over time when $v = 0$. Hence, if at some time $\bar{t}$, x has been driven to $\mathcal{C}_x$, control $v(t) = 0$, which corresponds to torque $u(t) = u_R$, keeps the trajectory inside $\mathcal{C}_x$ with acceleration $\tilde{a}(t)$ bounded above by the threshold value $\tilde{a}_{th}$, for all $t \geq \bar{t}$. The FFT control problem can then be formulated as the optimal control problem of steering the state x to manifold $\mathcal{C}_x$ in minimum time with $j \in [0, j_{\max}]$. Let $\mathcal{C}_\zeta$ be the image of $\mathcal{C}_x$ in the ζ state space

$$\mathcal{C}_\zeta \;=\; \left\{ \zeta \in \mathbb{R}^3 | \zeta = N_{\zeta x}^{-1} y - A^{-1}(b\, u_R - b_0) \text{ with } y \in \mathcal{C}_x \right\} \;. \qquad (4.1.15)$$

Problem 4.1.1 *Given the engine hybrid model $\mathcal{M}_{4cyl}$, for any ζ_0 not inside the region delimited by $\mathcal{C}_\zeta$ as in (4.1.15),*

$$\min_{\substack{\alpha \in \mathcal{A}_{4cyl} \\ \gamma \in \mathcal{G}_{4cyl} \\ \mathbf{r} \in \mathcal{R}_{4cyl}}} \int_0^T dt \qquad (4.1.16)$$

$$\textit{subject to:} \quad \begin{cases} \text{Dynamics of Hybrid Model } \mathcal{M}_{4cyl} \text{ with} \\ \textit{FSM initial state: } \mathcal{S}_1 = H, \mathcal{S}_2 = I, \mathcal{S}_3 = C, \mathcal{S}_4 = E, \\ z_1(0) = 0,\; z_2(0) = z_3(0) = z_4(0) = G q_0, \\ \zeta(0) = \zeta_0,\;\; \phi_c(0) = 0,\;\; p(0) = p_0 \\ \zeta(T) \in \mathcal{C}_\zeta \\ 0 \le j(t) \le j_{\max} \textit{ for all } t \in [0, T] \end{cases} \qquad (4.1.17)$$

with $(\zeta_0, 0)^T$ the powertrain dynamics state value at the initial time and p_0, $q_0 = c(\omega_c(0), p_0) p_0$ the corresponding manifold pressure and mass of air.

The above choice for the FSM initial state is not a limitation since any other admissible initial state can be obtained by a reordering of the cylinders.

4.2 FFT functional level design

In this Section the design of the functional level in the Fast Force Transient region is presented. At the functional level the plant is abstractly described relaxing the hybrid model $\mathcal{M}_{4cyl}$ to the continuous–time domain. Hence, the desired behavior is expressed by an optimal control problem which represents a relaxation of the original hybrid Problem 4.1.1. In Section 4.3, where the operation level design is described, relaxed problem solutions are mapped back to the hybrid domain yielding a sub–optimal solution to Problem 4.1.1. The relaxed problem is concerned with comfort requirements, for minimum time optimal trajectories of system (3.0.1) to manifold (4.1.15), assuming no constraint on torque signal. The solution is easily obtained by rewriting dynamics (3.0.1) with input j in place of u. From (3.0.1) and (3.0.4),

$$\dot{\zeta} \;=\; (I - b(cb)^{-1}c) A\, \zeta + (cb)^{-1} b\, j - (I - b(cb)^{-1}c) b_0 \;, \qquad (4.2.18)$$

$$u \;=\; -(cb)^{-1}(cA)\zeta + (cb)^{-1} j + (cb)^{-1}(c b_0) \;. \qquad (4.2.19)$$

System (4.2.18)-(4.2.19) corresponds to the inverse of system (3.0.1)-(3.0.4). For $a = c\,\zeta - d_0 = 0$, hence for $j = 0$ (4.2.18) represents the zero-dynamics of system (3.0.1)-(3.0.3), which has a pole in the origin and two poles equal to the zeros of $c(sI-A)^{-1}b$. Hence, it is characterized by one pole in the origin and two poles equal to the zeros of the system $c(sI-A)^{-1}b$. Since, c is proportional to the third row of A and the third entry in b is 0, $s=0$ is also a zero of $c(sI-A)^{-1}b$. Hence, dynamics (4.2.18) has two poles in the origin and a real pole η. A solution to the relaxed control problem is easily derived in the transformed space $\xi = N_{\zeta\xi}(\zeta + A^{-1}b\; u_R - A^{-1}b_0)$ of the natural modes,

$$\dot{\xi} \;=\; A_\xi \xi + b_\xi j \quad \text{with} \quad A_\xi = \begin{bmatrix} 0 & 1 & 0 \\ 0 & 0 & 0 \\ 0 & 0 & \eta \end{bmatrix} \tag{4.2.20}$$

where the target manifold is expressed as

$$\mathcal{C}_\xi \;=\; \left\{\xi \in \mathbb{R}^3 | \xi = N_{x\xi} x \text{ with } x \in \mathcal{C}_x\right\} \tag{4.2.21}$$

with $N_{x\xi} = N_{\zeta\xi} N_{\zeta x}^{-1}$. Let $\mathcal{J}$ denote the class of signals $j : \mathbb{R} \to [0, j_{\max}]$. The functional level relaxed control problem in the FFT region is:

Problem 4.2.1 *For any ξ_0 not inside the region delimited by $\mathcal{C}_\xi$ as in (4.2.21),*

$$\min_{j\in\mathcal{J}} \int_0^T dt \tag{4.2.22}$$

$$\textit{subject to:} \quad \begin{cases} \dot{\xi} = A_\xi\; \xi + b_\xi\; j \\ \xi(0) = \xi_0 \\ \xi(T) \in \mathcal{C}_\xi \end{cases} \tag{4.2.23}$$

The optimal solutions to Problem 4.2.1 are characterized as follows.

Proposition 4.2.1 *Let $\hat{j}(t)$, with $t \in [0,T]$, be an optimal solution to Problem 4.2.1 and let $\hat{\xi}(t)$ be the corresponding minimum time trajectory to manifold $\mathcal{C}_\xi$ as in (4.2.21). Then, $\hat{j}(t) \in \{0, j_{\max}\}$ for all $t \in [0,T]$ and*

$$\hat{j}(T) \;=\; \begin{cases} 0 & \text{if } b_\xi^T Q\xi(T) > 0 \\ j_{\max} & \text{if } b_\xi^T Q\xi(T) < 0 \end{cases}, \tag{4.2.24}$$

where $Q = N_2^T N_2 + N_3^T N_3$, with N_2, N_3 the second and third row of $N_{\xi x} = N_{x\xi}^{-1}$, respectively. Finally, there exist at most two times $t_1, t_2 \in [0,T]$ where a switching of $\hat{j}(t)$ takes place. These points are the solution of

$$[b_\xi^1 + b_\xi^2(T-t_i),\; b_\xi^2,\; b_\xi^3 e^{\eta(T-t_i)}]\; Q\xi(T) \;=\; 0,\; i=1,2\,. \tag{4.2.25}$$

The proof of the above proposition is obtained applying Pontryagin's Maximum Principle. The minimum time control to a given $\bar{\xi} = \xi(T) \in \mathcal{C}_\xi$

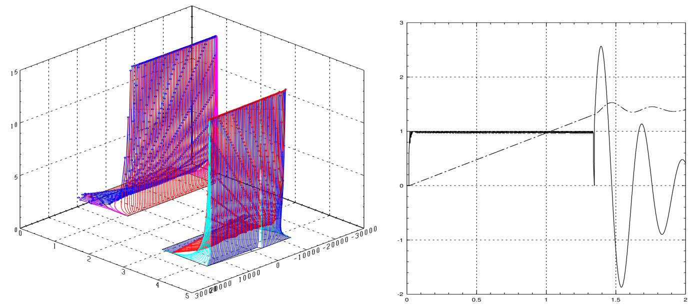

Figure 3: Switching surfaces in the minimum time control to $\mathcal{C}_x$ in cylindric coordinates (left). Acceleration and jerk profile in the hybrid closed loop system (right).

reachable in time T with jerk $j(\cdot) \in \mathcal{J}$, is derived as follows

$$\hat{j}(t) = \begin{cases} \hat{j}(T) \;\; \forall t \in [0,T] & \text{if (4.2.25) has no solution in } (0,T) \\ \begin{cases} j_{\max} - \hat{j}(T) & \forall t \in [0,t_1) \\ \hat{j}(T) & \forall t \in [t_1,T] \end{cases} & \text{if (4.2.25) has a solution } t_1 \in (0,T) \\ \begin{cases} \hat{j}(T) & \forall t \in [0,t_1) \\ j_{\max} - \hat{j}(T) & \forall t \in [t_1,t_2) \\ \hat{j}(T) & \forall t \in [t_2,T] \end{cases} & \text{if (4.2.25) has solutions } t_1, t_2 \in (0,T) \end{cases} \tag{4.2.26}$$

with $\hat{j}(T)$ as in (4.2.24). From any $\bar{\xi} \in \mathcal{C}_\xi$ reachable with $j(\cdot) \in \mathcal{J}$, the minimum time trajectory is obtained integrating backwards dynamics (4.2.20) with jerk signal as in (4.2.26). Let $\mathrm{Cont}(\mathcal{C}_\xi, T)$ denote the set of points controllable to $\mathcal{C}_\xi$, with $j(\cdot) \in \mathcal{J}$, in time lower than or equal to T. The backwards integration defines a partition $S_\xi^{j_{\max}}, S_\xi^0$ of set $\mathrm{Cont}(\mathcal{C}_\xi, T)$, such that for any $\xi \in \mathrm{Cont}(\mathcal{C}_\xi, T)$, the minimum time jerk control to $\mathcal{C}_\xi$ is expressed as

$$\hat{j}(\xi) \;=\; \begin{cases} 0 & \text{if } \xi \in S_\xi^0 \\ j_{\max} & \text{if } \xi \in S_\xi^{j_{\max}} \end{cases} . \tag{4.2.27}$$

From (4.2.19) and (4.2.27), the minimum time control to $\mathcal{C}_\zeta$ in the physical state space, in terms of torque on the crankshaft, is

$$\hat{u}(\zeta) = \begin{cases} (cb)^{-1}(-(cA)\zeta + (cb_0)), & \text{if } \zeta \in S_\zeta^0 \\ (cb)^{-1}(-(cA)\zeta + (cb_0) + j_{\max}), & \text{if } \zeta \in S_\zeta^{j_{\max}} \end{cases} \tag{4.2.28}$$

where $S_\zeta^{j_{\max}}$, S_ζ^0 are obtained mapping $S_\xi^{j_{\max}}$, S_ξ^0 to the ζ space.

4.3 FFT operation level design

The minimum time torque signal (4.2.28) is clearly not feasible for the hybrid model $\mathcal{M}_{4cyl}$ in Section 3. We derive in this Section an implementable approximation of torque (4.2.28), consistent with the hybrid model $\mathcal{M}_{4cyl}$, in terms of: throttle angle α, mix composition factor $\boldsymbol{\gamma}$, and spark modulation factor $\mathbf{r}$. The main difficulties are:

(a) available torque is limited to the set of values $\{0\} \cup G[r_{\min}\gamma_{\min}q, \gamma_{\max}q]$, where the air mass q is subject to manifold pressure dynamics;

(b) torque generation has to be synchronized with the powertrain dynamics;

(c) there is a delay between the time at which control signal γ_i (composition factor) and r_i (spark advance modulation) are set and the time at which the corresponding torque is generated.

To simplify discussion, set $\zeta(k) \stackrel{\triangle}{=} \zeta(t_k)$ for all k. As discussed in Section 3, the torque $u(k)$ provided by the $i-$th cylinder at time t_k depends on

1. the mass of air $q(k-2)$ loaded and the composition factor $\gamma_i(k-2)$ of the mix at time t_{k-2} (corresponding to an $H \to I$ transition of the $i-$th cylinder's FSM);
2. the spark modulation factor $r_i(k-1)$ applied at time t_{k-1} (corresponding to an $I \to C$ transition of the $i-$th cylinder's FSM).

Such torque feeds the powertrain dynamics in the interval $[t_k, t_{k+1})$, steering the state from $\zeta(k)$ to $\zeta(k+1)$. In order to properly set feedback signals γ_i and r_i, respectively at times t_{k-2} and t_{k-1}, a prediction of $\zeta(k)$ is needed at both instants. Assuming powertrain state available to measurement, one and two–step predictions are obtained by a forward integration of (3.0.1).

The torque generation process can be viewed as a MIMO system composed of two interconnected systems. The air mass evolution $q(t)$ is subject to manifold pressure dynamics (3.0.5), which is controlled by throttle angle α and depends on the crankshaft revolution speed ω_c. The torque to the crankshaft is provided by a two–step–delay discrete event system with inputs $\gamma_i(k)$ and $r_i(k)$. The coupling between the discrete event system and pressure dynamics is given by the driveline dynamics (3.0.1), through ω_c. While the impact on the discrete event system of q is not negligible, the driveline impact on air dynamics is weak enough to allow decentralization.

4.3.1 Air operation design

The reference evolution $\hat{q}(t)$ for air mass is obtained considering a rigid model for the driveline and solving the optimal control problem stated in the previous section assuming that $r_i = \gamma_i = 1$. Let τ_{drv} denote the driveline transmission ratio and let M_v denote the mass of the vehicle. In a rigid model of the driveline, the force acting on the vehicle is given by $\frac{u}{R\ \tau_{drv}}$ and $j = \frac{da}{dt} = (M_v\ R\ \tau_{drv})^{-1} \frac{du}{dt}$. A bound on the vehicle jerk limits the derivative of the torque. The reference signal $\hat{q}(t)$ is chosen as the one that yields the reference value u_R in minimum time for the rigid model, i.e.

$$\hat{q}(t) = \begin{cases} q(0) + j_{\max} \frac{M_v\ R\ \tau_{drv}}{G} t & \text{if } t < \frac{G(q_R - q(0))}{j_{\max} M_v R \tau_{drv}} \\ \\ q_R & \text{if } t \geq \frac{G(q_R - q(0))}{j_{\max} M_v R \tau_{drv}} \end{cases} \tag{4.3.29}$$

where $q_R = u_R/G$. A decentralized scheme in terms of the throttle angle for perfect tracking of (4.3.29) is devised using Variable Structure Control (VSC) technique (see [17]). Rewrite dynamics (3.0.5) as

$$\dot{p} = a_q(\omega_c, p)\, p + w \tag{4.3.30}$$

Consider $\hat{q}(t)$ as in (4.3.29) and introduce the function $\sigma(t) = q(t) - \hat{q}(t)$. By definition of $\hat{q}(t)$, $\hat{q}(t) = q(0)$ i.e. $\sigma(0) = 0$. The *equivalent control* is such signal w_{eq} which ensures $\sigma(t) = 0$ if $\sigma(0) = 0$. Imposing $\dot{\sigma} = 0$, from (3.0.6) and (4.3.30), the equivalent control is obtained as follows

$$w_{eq} \;=\; -a_q(\omega_c, p)\, p + \left(c_q(\omega_c, p) + \frac{\partial c_q}{\partial p}(\omega_c, p)\ p \right)^{-1} \left(\dot{\hat{q}} - \frac{\partial c_q}{\partial \omega_c}(\omega_c, p)\ p\ \dot{\omega}_c \right).$$

In practice, model (3.0.5), (3.0.6) is not perfectly known, so that one should modify control w_{eq} to cope with modeling uncertainties. Further, while $\dot{\hat{q}}$ is accessible, $\dot{\omega}_c$ is not available. However, driveline weak coupling allows to simplify the control by using a decentralized scheme (see [20],[16]). Interaction is compensated by a robust control with respect to nonlinearities and coupling (see e.g. [6]). Given a value $\bar{\eta}_v$, $\bar{\omega}_c$ of volumetric efficiency and crankshaft speed, introduce $a_{q1} = -\frac{V_d}{4\pi V_c} \bar{\eta}_v \bar{\omega}_c$, $c_{q1} = \frac{V_d}{4 R_g T_{atm}} \bar{\eta}_v$, and $\tilde{a}_q(\omega_c, p) = a_q(\omega_c, p) - a_{q1}$, $\tilde{c}_q(\omega_c, p) = c_q(\omega_c, p) - c_{q1}$. If $\tilde{a} = \tilde{c} = 0$, the VSC

$$w_{vsc} \;=\; -a_{q1}\ p + \frac{\dot{\hat{q}}}{c_{q1}} - \frac{W}{c_{q1}} \text{ sign } (\sigma) \tag{4.3.31}$$

with $W > 0$, guarantees a sliding regime along the manifold $\sigma(p, \hat{q}) = 0$, during which perfect tracking of reference signal $\hat{q}(t)$ is achieved.

Proposition 4.3.1 *Assume that* $p, \omega_c, \dot{\omega}_c, \dot{\hat{q}}$ *satisfy* $p \in [p_1, p_{atm}]$, $\omega_c \in [\omega_1, \omega_2]$, $|\dot{\omega}_c| \leq \dot{\omega}_{\max}$, $|\dot{\hat{q}}| \leq \dot{\hat{q}}_{\max}$. *Choose a* $\bar{\eta}_v$, $\bar{\omega}$ *and let* $\tilde{C}, \tilde{C}_p, \tilde{C}_{\omega_c}, \tilde{A}_q$ *be such that* $\tilde{C} \geq \max_{\omega_c, p} \left| \frac{\tilde{c}_q}{c_{q1}} \right|$, $\tilde{C}_p \geq \max_{\omega_c, p} \left| \frac{\partial \tilde{c}_q}{\partial p} \right|$, $\tilde{C}_{\omega_c} \geq \max_{\omega_c, p} \left| \frac{\partial \tilde{c}_q}{\partial \omega_c} \right|$, $\tilde{A}_q \geq \max_{\omega_c, p} |\tilde{a}_q|$. *Given* $\epsilon > 0$, *if* $\tilde{C} + \tilde{C}_p \frac{p_{atm}}{c_{q1}} < 1$ *the VSC (4.3.31) with*

$$W \;=\; c_{q1} \tilde{A}_q p_{atm} + \frac{\left(\tilde{C} + \tilde{C}_p\ \frac{p_{atm}}{c_{q1}} \right) \dot{\hat{q}}_{\max} + \left(\tilde{C}_{\omega_c}\ p_{atm} \right) \dot{\omega}_{\max} + \epsilon}{1 - \tilde{C} - \tilde{C}_p\ \frac{p_{atm}}{c_{q1}}} \tag{4.3.32}$$

guarantees a sliding motion on $\sigma = 0$, during which perfect tracking of $\hat{q}(t)$ as in (4.3.29) is achieved, robustly w.r.t. to driveline evolution.

A feedback in terms of throttle angle α is obtained from (4.3.31) by inverting the nonlinear input map $w = b_q(p)s(\alpha)$. In order to reduce the undesired chattering phenomena, typical in VSC, the sign function is replaced by $\frac{\sigma}{\delta+|\sigma|}$, where the smoothing parameter $\delta > 0$ is properly tuned so to maintain satisfactory tracking. The decentralized feedback is

$$\alpha \;=\; s^{-1}\left(\frac{1}{b_q(p)}\left(-a_{q1}\;p + \frac{\dot{\hat{q}}}{c_{q1}} - \frac{V}{c_{q1}}\;\frac{\sigma}{\delta+|\sigma|}\right)\right) \tag{4.3.33}$$

with $\sigma(t) = c_q(\omega_c, p)\;p - \hat{q}(t)$.

4.3.2 Motion generation operation design

A feedback in terms of mix composition factor $\gamma(k)$ and spark modulation factor $\mathbf{r}(k)$ which follows law (4.2.28) is presented in the sequel. Assuming that cranckshaft revolution speed does not change significantly between two successive FSM transitions in $\mathcal{M}_{4cyl}$, i.e. $t_{k+1} - t_k \approx \tau_k = \pi/\omega_c(t_k)$, since $u(t) = u(k)$ for $t \in [t_k, t_{k+1})$, powertrain dynamics (3.0.1),(3.0.3) is discretized as follows

$$\begin{aligned}\zeta(k+1) &= \hat{A}\zeta(k) + \hat{b}u(k) &\quad (4.3.34)\\ a(k) &= c\zeta(k) &\quad (4.3.35)\end{aligned}$$

where $\hat{A} = e^{A\,\tau_k}$, $\hat{b} = (\hat{A} - I)A^{-1}b$. The jerk mean value in the time intervall $[t_k, t_{k+1}]$ can be expressed as

$$\frac{\int_{t_k}^{t_{k+1}} j(t)dt}{t_{k+1}-t_k} = \frac{a(t_{k+1}) - a(t_k)}{t_{k+1}-t_k} \approx \frac{a(k+1)-a(k)}{\tau_k} = \frac{c(\hat{A}-I)}{\tau_k}\zeta(k) + \frac{c\hat{b}}{\tau_k}u(k).$$

Hence, the torque law

$$\hat{u}_d(k) \;=\; (c\hat{b})^{-1}c(\hat{A}-I)\zeta(k) + (c\hat{b})^{-1}\tau_k\;\hat{j}(\zeta(k))\;, \tag{4.3.36}$$

where $\hat{j}(\zeta)$ is chosen according to (4.2.27), that is

$$\hat{j}(\zeta) \;=\; \begin{cases} 0 & \text{if } \zeta \in S_\zeta^0 \\ j_{\max} & \text{if } \zeta \in S_\zeta^{j_{\max}} \end{cases} \tag{4.3.37}$$

produces a jerk with mean value equal to $\hat{j}(\zeta)$. The actual jerk profile in the evolution of the hybrid model $\mathcal{M}_{4cyl}$ exhibits a ripple on the average value due to the fact that, being $u(t)$ piecewise–constant, between two samples the natural modes of dynamics (3.0.1) evolve. Due to this ripple, jerk signal exceeds interval $[0, j_{\max}]$, and a more conservative feedback than (4.3.36) has to be devised.

Proposition 4.3.2 *Define*

$$\begin{aligned}
\hat{u}_c(\zeta) &= (cb)^{-1}(\hat{j}(\zeta) - cA\zeta) && (4.3.38)\\
\hat{u}_n(\zeta) &= (cA\hat{b} + cb)^{-1}(\hat{j}(\zeta) - cA\hat{A}\zeta) && (4.3.39)\\
\hat{u}_m(\zeta) &= (c(I + \tau_k A)b)^{-1}(j_{\max} - c(I + \tau_k A)A\zeta) && (4.3.40)
\end{aligned}$$

with $\hat{j}(\zeta)$ *as in (4.3.37). Let* $j_c(t)$,$j_n(t)$,$j_m(t)$ *and* $j_d(t)$ *denote the jerk profiles corresponding to torques (4.3.38), (4.3.39), (4.3.40) and (4.3.36) respectively. Assume that, under the feedback laws* $\hat{u}_c$,$\hat{u}_n$,$\hat{u}_m$ *and* $\hat{u}_d$, $\frac{d^2 j(t)}{dt^2} \leq 0$ *for all* $t \in [t_k, t_{k+1}]$. *The following control*

$$\hat{u}(k) = \begin{cases} \max(\hat{u}_c(\zeta), \hat{u}_n(\zeta)) & \text{if } \zeta(k) \in S_\zeta^0 \\ \begin{cases} \hat{u}_c(\zeta) & \text{if } j_d(t_k) > j_{\max} \wedge \frac{dj_c}{dt}(t_k) \leq 0 \\ \hat{u}_n(\zeta) & \text{if } j_d(t_{k+1}) > j_{\max} \wedge \frac{dj_n}{dt}(t_{k+1}) \geq 0 \\ \hat{u}_m(\zeta) & \text{otherwise} \end{cases} & \text{if } \zeta(k) \in S_\zeta^{j_{\max}} \end{cases} \qquad (4.3.41)$$

produces a jerk profile $j(t)$ *such that* $0 \leq j(t) \leq j_{\max}$.

A feedback control in terms of the mix composition factor $\gamma(k)$ of the cylinder which enters the I state, and the spark advance modulation $r(k)$ of the cylinder which enters the C state, which produces the torque $\hat{u}(k)$ as in (4.3.41), is reported in Figure 4. As discussed at the beginning of the section, control $\gamma(k)$ affects torque $u(k+2)$, while control $r(k)$ affects torque $u(k+1)$. The former depends also on the mass of air $q(k)$, while the latter depends on $q(k-1)$. Equation (4.3.41) gives the desired torque at time t_{k+1} and t_{k+2} in terms of future states $\zeta(k+1)$ and $\zeta(k+2)$ respectively. Figure 3 shows an evolution of jerk and acceleration in the hybrid system $\mathcal{M}_{4cyl}$ under the proposed feedback.

5 Fast Negative Force Transient design

5.1 The FNFT optimal control problem

For drive–by–wire cars, where the throttle valve is actuated by an electrical motor, the mass of air q is a regulated variable and the designer has full control on torque generation. For these systems the FNFT problem can be formulated as the FPFT problem where $u_R = 0$. The corresponding minimum time control problem is solved using the same arguments and algorithms described for the FPFT problem. However, for traditional systems, where the throttle valve is directly connected to the gas pedal and there is no possibility of acting on the mass of air loaded by the cylinders, a different approach has to be used. When the air quantity is not a controlled variable, the FNFT problem is typically referred to as the cut–off control problem, where the goal is to shut off fuel injection minimizing passengers' discomfort due to powertrain oscillations. In a cut–off operation, the

$\zeta_k = \zeta(t_k), \quad q_k = q(t_k)$ (current driviline state and mass of air)
$\tau_k = \pi/[0\ 1\ 0]\,\zeta_k, \quad \hat{A} = e^{A\,\tau_k}, \quad \hat{b} = (\hat{A} - I)A^{-1}b$ (current driviline discrete model)

$\zeta_{k+1} = \hat{A}\zeta(k) + \hat{b}\, z_2^c(k)$ (future driviline state)

if $\| N_{\zeta x}(\zeta_{k+1} + A^{-1} b u_R) \| > \hat{\rho}$ then (exit condition: state ζ in $\mathcal{C}_\zeta$)
    $\hat{u}_{k+1} = \hat{u}(k+1)$ (according to (4.3.41) evaluated at ζ_{k+1})
else
    $\hat{u}_{k+1} = u_R$ (target torque u_R applied)
endif

$r = \hat{u}_{k+1}/z_1^c(k)$
if $r < r_{\min}$ then $r = r_{\min}$ elseif $r > 1$ then $r = r_{\min}$ endif
$r(k) = r$ (spark advance control)

$\zeta_{k+2} = \hat{A}\zeta_{k+1} + \hat{b}\, r_k\, z_1^c(k)$ (next driviline state)
if $\zeta_{k+2} \in S_\zeta^0$ then
    $\hat{j} = 0$
endif

if $\| N_{\zeta x}(\zeta_{k+2} + A^{-1} b u_R) \| > \hat{\rho}$ then (exit condition: state ζ in $\mathcal{C}_\zeta$)
    $\hat{u}_{k+2} = \hat{u}(k+2)$ (according to (4.3.41) evaluated at ζ_{k+2})
else
    $\hat{u}_{k+2} = u_R$ (target torque u_R applied)
endif

$\gamma = \hat{u}_{k+2}/(G q_k)$
if $\gamma < \gamma_{\min}$ then $\gamma = \gamma_{\min}$ elseif $\gamma > \gamma_{\max}$ then $\gamma = \gamma_{\max}$ endif
$\gamma(k) = \gamma$ (mix composition control)

$z_1^c(k+1) = G\, q_k\, \gamma_k$ (next potential torque)
$z_2^c(k+1) = z_1^c(k)\, r$ (next predicted torque)

Figure 4: Discrete event algorithm for mix composition factor $\gamma(k)$ and spark advance modulation $r(k)$.

hybrid engine model $\mathcal{M}_{4cyl}$ is fed by a decreasing sequence $q_a(k)$ of air intakes, which converges to the steady-state air quantity with pedal released, q_a^o. This results in an upper bound for the available torque. We identify as the starting point of the cut–off control horizon the time $t_0 = t_{k_0}$ at which $q_a(k_0) = q_a(k_0 - 1) = q_a(k_0 - 2) = q_a^o$, i.e. the time at which all the loaded cylinders' potential torques are at the steady–state value. To simplify notation, we set $t_0 = 0$ and $k_0 = 0$, and we use u for v since $u_R = 0$.

The objective of cut–off control is to minimize the peak of the acceleration $\tilde{a}(t)$ until it is below the threshold of acceleration perception $\tilde{a}_{th}$. Remind that, once the powertrain state ζ is inside the region delimited by $\mathcal{C}_\zeta$ as in (4.1.15) (with $u_R = 0$), fuel injection can be shut off with vehicle oscillations below threshold. Hence, the cut–off control can be formulated as the optimal control problem of steering state ζ to $\mathcal{C}_\zeta$ minimizing the acceleration peaks, acting on the mix composition factor $\boldsymbol{\gamma}$ and the spark modulation factor $\mathbf{r}$ inputs.

Problem 5.1.1 *Given the engine hybrid model $\mathcal{M}_{4cyl}$, for any initial state ζ_0 not inside the region delimited by $\mathcal{C}_\zeta$ as in (4.1.15) (with $u_R = 0$),*

$$\min_{\substack{\boldsymbol{\gamma} \in \mathcal{G}_{4cyl} \\ \mathbf{r} \in \mathcal{R}_{4cyl}}} \ \sup_{0 \le t \le T} |\tilde{a}(t)|$$

$$\text{subject to:} \quad \begin{cases} \text{Dynamics of Hybrid Model } \mathcal{M}_{4cyl} \text{ with} \\ p(t) = p_0, \quad \text{for all } t \geq 0, \\ \textit{FSM initial state: } \mathcal{S}_1 = H, \mathcal{S}_2 = I, \mathcal{S}_3 = C, \mathcal{S}_4 = E, \\ z_1(0) = 0, \; z_2(0) = z_3(0) = z_4(0) = G q_a^o, \\ \zeta(0) = \zeta_0, \phi_c(0) = 0, \\ \zeta(T) \in \mathcal{C}_\zeta, \end{cases}$$

where $\tilde{a}(\cdot)$ is as in (4.1.13), p_0 is the steady-state manifold pressure with gas pedal released, i.e. $q_a^o = c_q(\omega_c(0), p_0)p_0$ and the final time $T < \infty$ is unspecified.

Note that, the above choice for the FSM initial state does not represent a limitation since any other admissible initial state can be obtained by a reordering of the cylinders.

5.2 FNFT functional level design

The main difficulties in Problem 5.1.1 are that the plant to be controlled is hybrid and that the input signals $\boldsymbol{\gamma}$ and $\mathbf{r}$ are bounded. The design at the functional level is developed relaxing the hybrid problem into the continuous–time domain, maintaining the bound on the value the torque signal u can take. In the operation level design the solution will be mapped back to the hybrid domain obtaining feedback laws in terms of the plant inputs $\boldsymbol{\gamma}$ and $\mathbf{r}$. Consider the transformed state space introduced in (4.1.10) associated with powertrain natural mode decomposition. Let

$$B_{\hat{\rho}} \;=\; \left\{ x \in \mathbb{R}^2 : \|x\| \leq \hat{\rho}, \quad \hat{\rho} = \tilde{a}_{th} \|c_x^T\|^{-1} \right\} \tag{5.2.42}$$

be the projection of the volume delimited by $\mathcal{C}_x$ as in (4.1.14) on the x sub-space. Since $u_R = 0$, we use u for v. The relaxed problem is as follows.

Problem 5.2.1 *Let*

$$\mathcal{U} = \{u : [0, +\infty) \to \mathbb{R} \mid u(t) \textit{ measurable and } 0 \leq u(t) \leq M, \forall t \geq 0\} \tag{5.2.43}$$

with $M = G\gamma_{\max} q_a^o$. For any initial state $x_0 \notin B_{\hat{\rho}}$ as in (5.2.42),

$$\min_{u \in \mathcal{U}} \sup_{0 \leq t \leq T} |\tilde{a}(t)|$$

$$\text{subject to:} \quad \begin{cases} \dot{x}(t) = A_x x(t) + b_x u(t) \\ x(0) = x_0 \\ x(T) \in \partial B_{\hat{\rho}} \end{cases}$$

where $\tilde{a}(\cdot)$ is as in (4.1.13) and the final time $T < \infty$ is unspecified.

Note that, for some initial conditions a solution to Problem 5.2.1 may not exist. In the sequel existence is discussed and a solution is given. Let

$R(\theta) \in \mathbb{R}^2$ be the counterclockwise rotation matrix of θ radians in $\mathbb{R}^2$ and, for any $x \in \mathbb{R}^2$, let $x_\perp$ denote $R(\frac{\pi}{2})x$. Let $x_M = -A_x^{-1} b_x M$ be the equilibrium point of (4.1.12) with $u = M$ and let $v = -\overrightarrow{vers}\,(x_M)_\perp$, where $\overrightarrow{vers}\,(x) \stackrel{\triangle}{=} \frac{x}{\|x\|}$. In our previous paper [2], it was shown that there exists $u \in \mathcal{U}$, which steers some initial states x_0 of (4.1.12) to the origin along a straight line (see Figure 5). However, under this control the time to reach $B_{\hat\rho}$ becomes unbounded as x_0 approaches the line $v^T x = 0$. We propose a modified control law that eliminates this problem by giving up (slightly) optimality for particular trajectories. However, optimality can be approached infinitely close as shown in the following theorem.

Theorem 5.2.1 *Consider an initial state $x_0 \notin B_{\hat\rho}$. Let $\mathcal{U}' \subset \mathcal{U}$ be the class of all input signals $u' \in \mathcal{U}$ which steer the state x of system (4.1.12) from x_0 to a point on $\partial B_{\hat\rho}$. Let $\psi(u', x_0, t)$, with $t \in [0, T]$, denote the trajectory from x_0 to $x_T = \psi(u', x_0, T) \in \partial B_{\hat\rho}$ corresponding to some $u' \in \mathcal{U}'$, where T depends on u' and x_0. Let*

$$\tilde{A}(x_0) = \inf_{u' \in \mathcal{U}'} \sup_{0 \le t \le T} |c_x \psi(u', x_0, t)| = \inf_{u' \in \mathcal{U}'} \sup_{0 \le t \le T} |\tilde{a}(t)| \Big|_{u=u'} .$$

For any $x \notin B_{\hat\rho}$, consider the feedback control

$$\hat{u} = \begin{cases} \begin{cases} 0 & \text{if } v^T x \ge 0 \\ M & \text{if } v^T x < 0 \end{cases} & \text{if } x \notin \mathcal{D}_M \\ \\ \begin{cases} -\frac{x^T R(-\frac{\pi}{2}) A_x x}{x^T R(-\frac{\pi}{2}) b} & \text{if } (R(\theta)v)^T x \le 0 \\ 0 & \text{if } (R(\theta)v)^T x > 0 \end{cases} & \text{if } x \in \mathcal{D}_M \end{cases} . \tag{5.2.44}$$

If $\|x_M\| \ge \hat\rho$ then

- **A1.** *if $(c_x x_M)(c_x b_x) > 0$ control (5.2.44) with θ set to any value in the interval $(0, \sin^{-1}(\frac{-\lambda}{\sqrt{\lambda^2+\mu^2}}))$, steers in finite time state x_0 to $\partial B_{\hat\rho}$ and is optimal for Problem 5.2.1, i.e. $\tilde{A}(x_0) = \sup_{0 \le t \le T} |\tilde{a}(t)| \big|_{u=\hat{u}}$.*

- **A2.** *if $(c_x x_M)(c_x b_x) \le 0$ there is a set of initial conditions $\mathcal{X}_0 \subset \mathbb{R}^2 / B_{\hat\rho}$ such that for any $x_0 \in \mathcal{X}_0$ no optimal solution in finite time exists. However, for any $\epsilon > 0$ there exists $\theta > 0$ such that control (5.2.44) steers any x_0 to $\partial B_{\hat\rho}$ in finite time with, $\sup_{0 \le t \le T} |\tilde{a}(t)| \big|_{u=\hat{u}} - \tilde{A}(x_0) < \epsilon$ if $x_0 \in \mathcal{X}_0$, and $\sup_{0 \le t \le T} |\tilde{a}(t)| \big|_{u=\hat{u}} = \tilde{A}(x_0)$ if $x_0 \notin \mathcal{X}_0$.*

else, if $\|x_M\| < \hat\rho$,

- **B.** *control (5.2.44) with $\theta = 0$, is optimal for Problem 5.2.1.*

It is interesting to note that for all models of existing cars available to us, $(c_x x_M)(c_x b_x) > 0$ and, hence, (5.2.44) was actually optimal. Figure 5 shows the closed loop phase space under control (5.2.44) with $(c_x x_M)(c_x b_x) > 0$ and $\theta \simeq 0$. The proof of Theorem 5.2.1 is based on the analysis of the reachable sets for system (4.1.12) with control $u \in \mathcal{U}$ (see [3],[4]).

5.3 FNFT operation level design

Torque signal (5.2.44) is clearly not feasible for the hybrid model $\mathcal{M}_{4cyl}$, introduced in Section 3. Following the approach illustrated in Section 4.3, feedback laws for the mix composition $\boldsymbol{\gamma}$ and the spark modulation $\mathbf{r}$, such that the produced torque approximates signal (5.2.44) are devised. Torque generation mechanism constraints described in Section 4.3, i.e. (a) bounds, (b) synchronization and (c) delay, have to be taken into account.

Our solution is to over–constrain the optimal control problem limiting our attention to bang–bang torque that can take the two extreme values 0 and M only. This corresponds to setting $r_i = 1$, and to using as feedback input γ_i which assumes values 0 (fuel not injected) and $\gamma_{\max}$ (maximum amount of fuel injected). Synchronization of γ_i, and hence of the generated torque, with the powertrain dynamics is the main difficulty. To compensate the torque generation 2-step delay, a prediction $\tilde{x}_2(k)$ of $x(t_{k+2})$ is obtained from $x(k)$ by forward integration of (4.1.12). The injection control is defined according to a switching curve $\sigma(x) = 0$, with $\sigma : \mathbb{R}^2 \to \mathbb{R}$ as follows

$$\hat{\gamma}_i(k) = \begin{cases} 0 & \text{if } \tilde{x}_2(k) \in B_{\hat{\rho}} \\ \begin{cases} 0 & \text{if } \sigma(\tilde{x}_2(k)) \geq 0 \\ 1 & \text{if } \sigma(\tilde{x}_2(k)) < 0 \end{cases} & \text{if } \tilde{x}_2(k) \notin B_{\hat{\rho}} \ . \end{cases} \tag{5.3.45}$$

In the sequel we assume that the prediction $\tilde{x}_2(k)$ is correct, i.e. $\tilde{x}_2(k) = x(t_{k+2})$. The bang-bang part of the control law for the continuous case is characterized by the switching line

$$\sigma(x) = v^T x. \tag{5.3.46}$$

It is natural to propose this bang-bang control for the hybrid case. However, convergence of this bang–bang control law is not obvious. The properties of (5.3.45) depend on the position of x_M with respect to $B_{\hat{\rho}}$. If $\|x_M\| \leq \hat{\rho}$, control law (5.3.45), with $\sigma(x)$ as in (5.3.46), has been proven to yield trajectories that converge to $B_{\hat{\rho}}$ if the engine speed is larger than an appropriate bound (see [4]). If $\|x_M\| > \hat{\rho}$, we have shown that this control law may not converge and $\sigma(x)$ needs to be modified to guarantee convergence. Since for all model parameters seen in commercial cars $\|x_M\| > \hat{\rho}$, we discuss only this case.

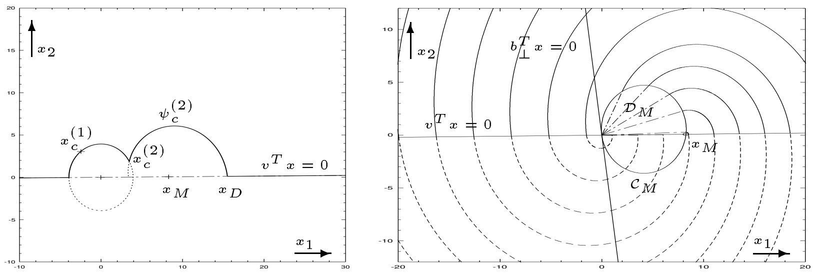

Figure 5: Optimal trajectories for the relaxed problem. If $x \notin \mathcal{D}_M$, u is equal to either M (solid line) or 0 (dashed line). Otherwise $0 < u < M$ (dash-dot line). Hybrid switching line for $\|x_M\| > \rho$.

5.3.1 Convergence analysis and performances

Since $\|x(t)\|$ monotonically converges to zero when torque $u = 0$ is applied, we need to worry only when the generated torque under feedback (5.3.45) continues to be $u = M$, while the continuous torque feedback (5.2.44) calls for $u = 0$. The set of points such that a torque $u = M$ applied for time Δ causes an increase in norm is $\bar{\mathcal{N}}_\Delta = \{x \in \mathbb{R}^2 \mid \|x\| < \|e^{A_x\Delta}(x - x_M) + x_M\|\}$. Since $\lim_{\Delta\to 0} \bar{\mathcal{N}}_\Delta \neq \bar{\mathcal{N}}_\Delta\big|_{\Delta=0}$, $\bar{\mathcal{N}}_\Delta$ is extended by continuity as follows

$$\mathcal{N}_\Delta = \begin{cases} \bar{\mathcal{N}}_\Delta & \text{if } \Delta > 0, \\ \{x \in \mathbb{R}^2 \mid x^T A_x (x - x_M) \geq 0\} & \text{if } \Delta = 0. \end{cases} \tag{5.3.47}$$

Define the sequence $\Delta_k \stackrel{\triangle}{=} t_{k+1} - t_k$. If $\Delta_k = \frac{\pi}{\mu}$ the generated torque under feedback (5.3.45) switches to 0 when it should switch to M and vice versa and the resulting performance is poor. We restrict engine speed to $\omega_c(t) > 2\mu$ for all $t > 0$, i.e. $\Delta_k < \frac{\pi}{2\mu}$ for all $k > 0$. For all Δ' such that $\partial B_{\hat\rho} \cap \partial \mathcal{N}_{\Delta'} = \emptyset$, $B_{\hat\rho} \subset \mathcal{N}_{\Delta'}$. Thus trajectories with $\omega_c(t) \leq \frac{\pi}{\Delta'}$ for some t, may "jump" $B_{\hat\rho}$ under $u(k) = M$. Hence, to prevent this undesirable behavior, the switching line is defined considering the intersections between $\partial\mathcal{N}_\Delta$ and $\partial B_{\hat\rho}$.

Lemma 5.3.1 *There exists $\Delta_{\mathcal{N}} > 0$ such that for all $\Delta \in [0, \Delta_{\mathcal{N}})$,*

$$\partial\mathcal{N}_\Delta \cap \partial B_{\hat\rho} = \{x_c^{(1)}, x_c^{(2)}\} \textit{ with } x_c^{(1)} \neq x_c^{(2)}, \;\; x_M(x_c^{(2)} - x_c^{(1)}) > 0. \tag{5.3.48}$$

Let $\Delta_{\mathcal{N}}^0 = \min\{\frac{\pi}{2\mu}, \Delta_{\mathcal{N}}\}$. Assume that the crankshaft velocity satisfy $\omega_c(t) > \frac{\pi}{\Delta}$ for all $t > 0$, for some $\Delta < \Delta_{\mathcal{N}}^0$, so that $\partial B_{\hat\rho} \cap \partial\mathcal{N}_\Delta \neq \emptyset$.

Consider point $x_c^{(2)}$ as in (5.3.48) and introduce the arc $\psi_c^{(2)}$ from x_D to $x_B = \psi(M, x_D, \pi/\mu)$ such that $v^T x_D = v^T x_B = 0$ and $x_c^{(2)} \in \psi_c^{(2)}$, i.e.,

$$\psi_c^{(2)} = \left\{x \in \mathbb{R}^2 | x = \psi(M, x_D, \tau) \text{ with } \tau \in [0, \pi/\mu]\right\}. \tag{5.3.49}$$

The switching function (5.3.46) is modified to include the arc $\psi_c^{(2)}$:

$$\sigma(x) = \begin{cases} (v^T b_x/\|b_x\|)^{-1} v^T x, & \text{if } ({b_{x\perp}}^T x \leq {b_{x\perp}}^T x_B) \vee \\ & \quad ({b_{x\perp}}^T x \geq {b_{x\perp}}^T x_D) \\ (b_x/\|b_x\|)^T (x - x_b), & \text{if } {b_{x\perp}}^T x_B < {b_{x\perp}}^T x < {b_{x\perp}}^T x_D \\ \text{with } x_b \text{ s.t. } ({b_{x\perp}}^T (x - x_b) = 0) \ \wedge (\ x_b \in \psi_c^{(2)}) \end{cases} \tag{5.3.50}$$

Note that, since $x_c^{(2)}$ depends on Δ, $\sigma(x)$ is chosen conservatively based on the lower bound for the crankshaft speed ω_c. Let $\varphi(\hat{\gamma}_i, x_0, t)$ denote a generic trajectory in the reduced state space x obtained under control (5.3.45) with $x(0) = x_0$.

Proposition 5.3.1 *Assume $\omega_c(t) > \omega_1$ for all $t \geq 0$ (with $\omega_1 \geq \frac{\pi}{\Delta^0_{\mathcal{N}}}$) and consider all trajectories $\varphi(\hat{\gamma}_i, x_0, t)$ under control $\hat{\gamma}_i(k)$ as in (5.3.45) with $\sigma(x)$ as in (5.3.50) with $\Delta = \frac{\pi}{\omega_1}$. There exists engine speed $\omega_{\min}$ such that, if $\omega_1 > \omega_{\min}$, for all initial conditions x_0 trajectories $\varphi(\hat{\gamma}_i, x_0, t)$ converge to $B_{\hat{\rho}}$ in finite time.*

The proof reported in [4] is constructive and gives the value $\omega_{\min}$. An optimal solution to Problem 5.1.1 is unknown, however bounds on the attainable cost can be obtained comparing the relaxed problem optimal solution cost to the cost attainable by the proposed hybrid control, thus proving the quality of the approach.

Given $x_0 \notin B_{\hat{\rho}}$, let $\psi(\hat{u}, x_0, t)$ denote the closed loop trajectory in the reduced state space under relaxed optimal torque control $\hat{u}(t)$ as in (5.2.44) from x_0 to $\partial B_{\hat{\rho}}$. Let $\bar{T}$ be such that $\psi(\hat{u}, x_0, \bar{T}) \in \partial B_{\hat{\rho}}$ and let $\bar{x} = \psi(\hat{u}, x_0, \bar{t})$, with $\bar{t} \in [0, \bar{T}]$, be such that $|c_x \bar{x}| = \max_{t \in [0,\bar{T}]} |c_x \psi(\hat{u}, x_0, t)|$. Let $\hat{T}$ denote the time needed to steer under control $\hat{\gamma}_i(k)$ as in (5.3.45) the initial state x_0 to $\partial B_{\hat{\rho}}$, i.e. $\varphi(\hat{\gamma}_i, x_0, \hat{T}) \in \partial B_{\hat{\rho}}$. Let $\hat{x} = \varphi(\hat{\gamma}_i, x_0, \hat{t})$, with $\hat{t} \in [0, \hat{T}]$, be such that $|c_x \hat{x}| = \max_{t \in [0,\hat{T}]} |c_x \varphi(\hat{\gamma}_i, x_0, t)|$.

Proposition 5.3.2 *(See [4].) Assume $\omega_c(t) > \omega_{\min} = \frac{\pi}{\Delta_{\max}}$ $\forall t \geq 0$, where $\omega_{\min}$ is given by Proposition 5.3.1. If $(c_x x_M)(c_x b_x) > 0$, there exists $\rho_w > 0$ such that, given x_0 with $\|x_0\| > \rho_w$, the following holds:*

$$0 \leq |c_x \hat{x}| - |c_x \bar{x}| \leq w_a^0(-\rho^0 v_\perp, \Delta_{\max}) \qquad \text{if } v^T x_0 < 0$$

$$0 \leq |c_x \hat{x}| - |c_x \bar{x}| \leq w_a^M(\rho^M, v_\perp, \Delta_{\max}) \qquad \text{if } v^T x_0 \geq 0$$

where $\rho^0 = \rho_w e^{\frac{\pi\lambda}{\mu}} - \|x_M\| \left(1 + e^{\frac{\pi\lambda}{\mu}}\right)$, $\rho^M = \rho_w e^{\frac{\pi\lambda}{\mu}}$,

$$\begin{aligned} w_a^0(x, \Delta) &= |c_x h_\perp| (\|\psi(0, x_a^0, \mu\angle(x_a^0, h_\perp))\| - \|\psi(0, x, \mu\angle(-v, h))\|) \\ w_a^M(x, \Delta) &= |c_x h_\perp| \left(\|\psi(M, x_a^M, \mu\alpha^M)\| - \|\psi(M, x, \mu\angle(-v, h))\|\right) \end{aligned}$$

where $h = \overrightarrow{vers}\left((cA_x)^T\right)$, $x_a^0 = \psi(M, x, \Delta)$, $x_a^M = \psi(0, x, \Delta)$ *and* $\alpha^M = \angle((x_a^M - x_M), -h_\perp)$.

If x_0 *belongs to either* $\mathcal{R}_3 = \left\{x \in \mathbb{R}^2 \mid v^T x < 0,\, (c_x x_M) h^T (x - x_M) < 0\right\}$ *or* $\mathcal{R}_4 = \left\{x \in \mathbb{R}^2 \mid v^T x > 0,\, (c_x x_M) h^T x > 0\right\}$ *the hybrid control (5.3.45) is optimal for Problem 5.1.1.*

5.4 Experimental results

The proposed cut–off control strategy has been implemented and tested at Magneti-Marelli Engine Control Division on a commercial car, a 16 valve 1400 cc engine car. The engine control electronics is a 4LV Magneti Marelli on board computer based on a 25MHz 32–bit Althair Motorola microprocessor with fixed point arithmetic unit. The experiment was carried out driving the car in the test ring and measuring the important parameters and variables that determine the performance of the control strategy.
The convergence analysis for the nominal values of the parameters, ensures convergence for engine speeds greater than $\omega_{\min} \simeq 396$ rpm. To prevent engine from stopping, cut-off strategies are usually not applied for ω_c less than 1000 rpm. The proposed control requires knowledge of the powertrain state. The problem of devising a robust observation scheme for the powertrain dynamics in any operating condition is out of the scope of this paper and is a topic currently under investigation. In our experiments, a discrete-time Luenberger observer has been shown to perform satisfactorily. In Figures 6 the performance achieved by the proposed cut-off strategy are compared with the performance of a currently implemented open-loop strategy. On the left, the evolutions in the $\hat{x}$ sub–space of the observer are reported along with the switching curve $\sigma(x) = 0$, as it is approximated in the implementation, and the target set $B_{\hat{\rho}}$. On the right, the resulting evolutions of the oscillating component $\tilde{a}(t)$ of the acceleration are shown. With the proposed control strategy the state is steered to $B_{\hat{\rho}}$ with no encirclement and $\tilde{a}(t)$ monotonically decreases to a_{th}. As expected from the theoretical results, once injection is set to zero permanently $\tilde{a}(t)$ remains bounded within the perception threshold. In the open-loop strategy an encirclement of $B_{\hat{\rho}}$ produces a peak of the acceleration.

6 Conclusions

We have presented a top-down methodology for the design of embedded controllers for automotive applications, that encompasses all levels of design abstractions from specifications to final implementation. In this paper, we focussed on the highest levels of abstraction, i.e. at the specification level and at the control algorithm design level. At these levels we made use of an abstract model of the plant (engine and drive-line) that hides details unnecessary for the synthesis of the control algorithms. The abstract

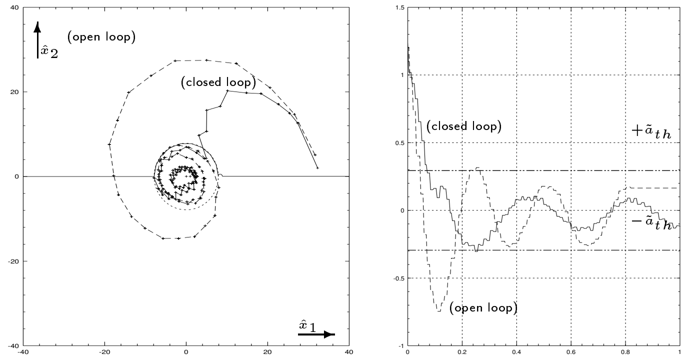

Figure 6: Observer sub-space $\hat{x}$ evolution with target set $B_{\hat{\rho}}$ and switching line $\sigma(x) = 0$ (on the left) and oscillating acceleration (in m/second^2) $\tilde{a}(t)$ signal profiles (on the right), in a controlled cut–off (solid line) and an uncontrolled cut-off (dashed line).

model represents the torque generation process as a finite-state machine and the drive-line as a third order system of ordinary differential equations. Hence, the control problems are cast in the hybrid system frame. Two important sub-problems have been considered corresponding to two specific regions of operations of the engine: Fast Positive and Fast Negative Force Tracking. For both problems, we derived a quasi-optimal control law by solving a relaxed problem in the continuous domain and then mapping back the solution in the hybrid space. Because of the particular aspects of our model, we have been able to bound rigorously the deterioration in performance of the control law with respect to the super-optimal strategy derived for the relaxed problem. This scheme appears to be extensible to all regions of operation of the engine thus providing a general paradigm for the entire engine control problem. We expect to conclude the design of the complete engine controller by the end of 1998. The successive step of mapping the algorithms into a computing architecture is carried out using a design methodology that is the basis of the Polis system developed at the University of California at Berkeley [1] and incorporated in the Felix VCC environment by Cadence Design Systems, Inc.

7 Acknowledgments

This research has been partially sponsored by PARADES, a Cadence, Magneti-Marelli and SGS-Thomson GEIE, and by CNR. We wish to acknowledge the support of the management of Magneti Marelli, and, in particular of Drs. Rossi, who pointed the cut-off problem out as a challenge, Pecchini, Mortara and Romeo. ISI provided the X-Math environment to carry out the simulation and the development of the control law.

Dr. Alberto Ferrari developed two powerful simulation environments, both including X-Math. One is based on Ptolemy, a University of California simulation and design tool for heterogeneous systems, the other on BoNES, a commercial simulation tool from the Alta group of Cadence; these environments have been essential to develop, tune and implement the control strategies. Dr. Luca Benvenuti offered insightful comments on the results of the paper.

References

[1] F. Balarin, M. Chiodo, P. Giusto, H. Hsieh, A. Jurecska, L. Lavagno, C. Passerone, A. Sangiovanni-Vincentelli, E. Sentovich, K. Suzuki, and B. Tabbara, *Hardware-software co-design of embedded systems, the polis approach*, VLSI, Computer Architecture and Digital Signal Processing, Kluwer Academic Publishers, Boston, Dordrecht, London, 1997.

[2] A. Balluchi, M. Di Benedetto, C. Pinello, C. Rossi, and A. Sangiovanni-Vincentelli, *Cut-off in engine control: a hybrid system approach*, 36th CDC (San Diego, CA), 1997, pp. 4720–4725.

[3] ———, *Hybrid control for automotive engine management: The cut-off case.*, Hybrid Systems: Computation and Control (T. A. Henzinger and S. Sastry, eds.), Lecture Notes in Computer Science, vol. 1386, Springer–Verlag, London, U.K., 1998, pp. 13–32.

[4] ———, *Hybrid control in automotive applications: the cut-off control.*, Tech. Report No. M98/34, UCB ERL, June 1998.

[5] K. Butts, I. Kolmanovsky, N. Sivashankar, and J. Sun, *Hybrid systems in automotive control applications*, Control using logic–based switching (A. S. Morse, ed.), Lecture notes in control and information sciences, vol. 222, Springer–Verlag, London, U.K., 1997, pp. 173–189.

[6] Y.H. Chen, G. Leitmann, and Z.K. Xiong, *Robust control design for interconnected systems with time–varying uncertainties*, Inter. J. Contr. **54** (1991), 1119–1142.

[7] X. Ge, W. Kohn, A. Nerode, and J. B. Remmel, *Hybrid systems: Chattering approximation to relaxed controls*, Hybrid Systems III (R. Alur, T. Henzinger, and E. D. Sontag, eds.), Lecture Notes in Computer Science, vol. 1066, Springer–Verlag, London, U.K., 1996, pp. 76–100.

[8] C. Horn and P. J. Ramadge, *Robustness issues for hybrid systems*, 34th CDC (New Orleans, LA), 1995, pp. 1467–1472.

[9] L. Hou, A. Michel, and H. Ye, *Stability analysis of switched systems*, 35th CDC (Kobe, Japan), 1996, pp. 1208–1212.

[10] W. Kohn, A. Nerode, and J. B. Remmel, *Hybrid systems as Finsler manifolds: Finite state control as approximation to connections*, Hybrid Systems II (P. Antsaklis, W. Kohn, A. Nerode, and S. Sastry, eds.), Lecture Notes in Computer Science, vol. 999, Springer–Verlag, London, U.K., 1995, pp. 294–321.

[11] E. Lee and A. Sangiovanni-Vincentelli, *Comparing models of computation*, Proc. International Conference on CAD (Santa Clara, CA), 1996, pp. 234–241.

[12] A. S. Morse (ed.), *Control using logic–based switching*, Lecture notes in control and information sciences, vol. 222, Springer–Verlag, London, U.K., 1997.

[13] A. Nerode and W. Kohn, *Models for hybrid systems: Automata, topologies, controllability, observability*, Hybrid Systems (R. L. Grossman, A. Nerode, A. P. Ravn, and Hans Rishel, eds.), Lecture Notes in Computer Science, vol. 736, Springer–Verlag, London, U.K., 1993, pp. 317–356.

[14] T. Niinomi, B. H. Krogh, and J. E. R. Cury, *Synthesis of supervisory controllers for hybrid systems based on approximating automata*, 34th CDC (New Orleans, LA), 1995, pp. 1461–1466.

[15] S. Pettersson and B. Lennartson, *Stability and robustness for hybrid systems*, 35th CDC (Kobe, Japan), 1996, pp. 1202–1207.

[16] H. H. Rosenbrock, *Computer-aided control system design*, Academic Press, London, U.K., 1974.

[17] V.I. Utkin, *Variable structure systems with sliding modes: a survey*, IEEE Trans. on Aut. Contr. **22** (1977), 212–222.

[18] L. Y. Wang, A. Beydoun, J. Cook, J. Sun, and I. Kolmanovsky, *Optimal hybrid control with applications to automotive powertrain systems*, Control using logic–based switching (A. S. Morse, ed.), Lecture notes in control and information sciences, vol. 222, Springer–Verlag, London, U.K., 1997, pp. 190–200.

[19] Hui Ye, A. N. Michel, and L. Hou, *Stability theory for hybrid dynamical systems*, 34th CDC (New Orleans, LA), 1995, pp. 2679–2684.

[20] L. F. Yeung and G. F. Bryant, *New dominance concepts for multivariable control systems design*, Inter. J. Contr. **55** (1992), no. 4, 969–988.

PARADES G.E.I.E., Via San Pantaleo, 66, 00186 Roma, Italy

Dipartimento di Ingegneria Elettrica, Università dell'Aquila, Poggio di Roio, 67040 L'Aquila, Italy

PARADES G.E.I.E., Via San Pantaleo, 66, 00186 Roma, Italy

Department of Electrical Engineering and Computer Science, University of California at Berkeley, CA 94720, USA; PARADES G.E.I.E., Via San Pantaleo, 66, 00186 Roma, Italy